Endocrinology, 2024, **165**, bqae057
https://doi.org/10.1210/endocr/bqae057
Advance access publication 10 May 2024
Research Article

The Pattern of GH Action in the Mouse Brain

Filipe Menezes,[1] Frederick Wasinski,[2,3] Gabriel O. de Souza,[2] Amanda P. Nunes,[1] Emerson S. Bernardes,[4] Sofia N. dos Santos,[4] Fábio F. A. da Silva,[4] Cibele N. Peroni,[1] João E. Oliveira,[1] John J. Kopchick,[5] Rosemary S. E. Brown,[6] Gimena Fernandez,[7] Pablo N. De Francesco,[7] Mario Perelló,[7,8] Carlos R. J. Soares,[1] and Jose Donato Jr[2]

[1]Biotechnology Center, Instituto de Pesquisas Energéticas e Nucleares, IPEN-CNEN/SP, São Paulo 05508-000, Brazil
[2]Departamento de Fisiologia e Biofísica, Instituto de Ciencias Biomedicas, Universidade de Sao Paulo, Sao Paulo 05508-000, Brazil
[3]Department of Neurology and Neurosurgery, Federal University of Sao Paulo, Sao Paulo 04039-032, Brazil
[4]Radiopharmacy Center, Instituto de Pesquisas Energéticas e Nucleares, IPEN-CNEN/SP, São Paulo 05508-000, Brazil
[5]Edison Biotechnology Institute and Heritage College of Osteopathic Medicine, Ohio University, Athens, OH 45701, USA
[6]Department of Physiology, Centre for Neuroendocrinology, School of Biomedical Sciences, University of Otago, Dunedin 9054, New Zealand
[7]Laboratory of Neurophysiology, Multidisciplinary Institute of Cell Biology, La Plata, BA 1900, Argentina
[8]Department of Surgical Sciences, Functional Pharmacology and Neuroscience, University of Uppsala, Uppsala 75312, Sweden

Correspondence: Jose Donato Jr, PhD, Instituto de Ciencias Biomedicas, Universidade de Sao Paulo, Av. Prof. Lineu Prestes, 1524, São Paulo 05508-000, Brazil. Email: jdonato@icb.usp.br.

Abstract

GH acts in numerous organs expressing the GH receptor (GHR), including the brain. However, the mechanisms behind the brain's permeability to GH and how this hormone accesses different brain regions remain unclear. It is well-known that an acute GH administration induces phosphorylation of the signal transducer and activator of transcription 5 (pSTAT5) in the mouse brain. Thus, the pattern of pSTAT5 immunoreactive cells was analyzed at different time points after IP or intracerebroventricular GH injections. After a systemic GH injection, the first cells expressing pSTAT5 were those near circumventricular organs, such as arcuate nucleus neurons adjacent to the median eminence. Both systemic and central GH injections induced a medial-to-lateral pattern of pSTAT5 immunoreactivity over time because GH-responsive cells were initially observed in periventricular areas and were progressively detected in lateral brain structures. Very few choroid plexus cells exhibited GH-induced pSTAT5. Additionally, *Ghr* mRNA was poorly expressed in the mouse choroid plexus. In contrast, some tanycytes lining the floor of the third ventricle expressed *Ghr* mRNA and exhibited GH-induced pSTAT5. The transport of radiolabeled GH into the hypothalamus did not differ between wild-type and dwarf *Ghr* knockout mice, indicating that GH transport into the mouse brain is GHR independent. Also, single-photon emission computed tomography confirmed that radiolabeled GH rapidly reaches the ventral part of the tuberal hypothalamus. In conclusion, our study provides novel and valuable information about the pattern and mechanisms behind GH transport into the mouse brain.

Key Words: blood-brain barrier, circumventricular organs, GH, hypothalamus, neuroendocrinology

Abbreviations: AgRP, agouti-related protein; AP, area postrema; ARH, arcuate nucleus of the hypothalamus; BBB, blood-brain barrier; CSF, cerebrospinal fluid; CVO, circumventricular organ; DMH, dorsomedial nucleus of the hypothalamus; GHR, GH receptor; hGH, human GH; ICV, intracerebroventricular; KPBS, potassium PBS; ME, median eminence; mGH, mouse GH; NTS, nucleus tractus solitarii; NPY, neuropeptide Y; OVLT, organum vasculosum of the lamina terminalis; pGH, GH extracted from porcine pituitary; PrlR, prolactin receptor; pSTAT5, phosphorylation of the signal transducer and activator of transcription 5; PV, periventricular nucleus; PVH, paraventricular nucleus of the hypothalamus; SPECT-CT, single-photon emission computed tomography; VMH, ventromedial nucleus of the hypothalamus; WT, wild-type.

Hypothalamic neurons are responsible for secreting stimulatory or inhibitory factors to control the synthesis and release of different pituitary hormones (1, 2). These hypothalamic neurohormones are secreted in the median eminence (ME), a circumventricular organ (CVO) (3). From the ME vessels, hypothalamic neurohormones reach endocrine cells of the anterior pituitary gland via the hypophyseal portal system (1, 2). On the other hand, the fenestrated capillaries of the ME allow the diffusion of circulating substances to nearby glial and neuronal populations in the hypothalamus. Schaeffer et al (4) showed that molecules with a molecular size of 20 kDa or less can freely extravasate through fenestrated vessels of the ME, whereas molecules with a molecular size of 40 kDa or more show no in vivo extravasation. Thus, the molecule size permeability cutoff of the ME is between 20 and 40 kDa (4). Cells near other CVOs, such as the organum vasculosum of the lamina terminalis (OVLT) and the area postrema (AP), are also targeted by circulating hormones without the typical limitations of the blood-brain barrier (BBB).

The arcuate nucleus of the hypothalamus (ARH) is adjacent to the ME, making ARH cells susceptible to variations of different circulating factors (4, 5). This is particularly important for neurons that coexpress the agouti-related protein (AgRP) and neuropeptide Y (NPY) because these cells are located in the ventromedial ARH; thus, they are the closest to the ME (5). Previous studies confirmed that a subpopulation of

Received: 7 February 2024. **Editorial Decision:** 7 May 2024. **Corrected and Typeset:** 30 May 2024

$ARH^{AgRP/NPY}$ neurons is outside the BBB (5). This feature makes $ARH^{AgRP/NPY}$ neurons susceptible to circulating factors. For example, $ARH^{AgRP/NPY}$ neurons need only a few days to be affected by a pro-inflammatory diet, developing leptin resistance earlier than other neuronal populations (5). In accordance with these findings, the activity of $ARH^{AgRP/NPY}$ neurons is modulated by pro-inflammatory cytokines, such as TNF-α and IL-1β (6).

The interaction between the ARH and ME makes ARH neurons especially effective in detecting variations in circulating factors (eg, nutrients, hormones) to control aspects such as food intake, body weight, energy metabolism, and glucose homeostasis (7, 8). ARH neurons express receptors for numerous hormones that control energy homeostasis, including leptin, ghrelin, cholecystokinin, glucagon-like peptide-1, and insulin (7, 8), all of which can readily reach ARH neurons after crossing the fenestrated capillaries of the ME (4). However, evidence suggests that protein transport is necessary to facilitate the normal diffusion of several peptide hormones to the hypothalamus. This transport can be mediated by hormone receptors expressed by brain vascular endothelial cells or tanycytes (9-12). Tanycytes are a hypothalamic ependymoglial cell type located on the ventral part of the third ventricle forming a blood-cerebrospinal fluid (CSF) barrier (13) that controls the transport of molecules between the blood and the hypothalamus or CSF (12). Thus, receptors can bind their specific ligands on one side of these cells and transport them to the other cell side.

In recent years, the role of hormone receptors in tanycytes in mediating the transport of different peptide hormones to the hypothalamus and CSF has been demonstrated. Thus, the availability of leptin (14, 15), insulin (16), and glucagon-like peptide-1 agonists (17) to the hypothalamus relies on tanycytes that express their cognate receptors. However, ghrelin access to the brain partially depends on a mechanism via choroid plexus cells, another cell type involved in the blood-CSF barrier (18). This transport is partially ghrelin receptor-dependent and can also occur in the absence of ghrelin receptor (19, 20). The pituitary hormone prolactin also accesses the brain via a mechanism independent of the prolactin receptor (PrlR) (21). Thus, several mechanisms are involved in transporting different protein hormones into the brain.

GH is a 191-amino acid, single-chain polypeptide (20-23 kDa, depending on the variant) secreted by somatotropic cells of the anterior pituitary gland. Although the most well-known effects of GH involve the activation of the GH receptor (GHR) in tissues such as the liver, adipose tissue, muscle, and pancreas (22), numerous brain areas express GHR. Thus, GH presumably diffuses into the brain and binds to its receptors in these areas (23). Accordingly, systemic GH injection induces the activation of GHR signaling pathways in the brain (24-26), particularly tyrosine phosphorylation of the signal transducer and activator of transcription 5 (pSTAT5), which is then translocated to the nucleus and acts as a critical transcription factor. Among all neural populations responsive to GH (27), $ARH^{AgRP/NPY}$ neurons are particularly relevant because *Ghr* mRNA expression is highly enriched in these cells (28). Histological studies found that 95% of $ARH^{AgRP/NPY}$ neurons express *Ghr* mRNA (29, 30) or exhibit pSTAT5 after an IP GH injection (31). GHR ablation in $ARH^{AgRP/NPY}$ neurons affects food intake (32), energy expenditure (31), thermogenesis (33), and developmental aspects of these cells (34).

Some evidence indicates that GH enters the mouse brain without a saturable transport system, suggesting simple diffusion (35). Another study showed that GH crosses the BBB and accumulates in different brain areas of chicken embryos (36). Although the brain, particularly the hypothalamus, contains numerous GH-responsive neuronal populations (24, 26), it is currently unknown how GH enters the central nervous system and diffuses through the brain's parenchyma. Thus, the objective of the present study is to investigate the transport of GH into the mouse brain using histological and pharmacological approaches. Dwarf *Ghr* knockout ($Ghr^{-/-}$) mice were used to examine whether GHR is necessary for GH transport into the brain.

Materials and Methods

Animals

The current study used male and female C57BL/6J wild-type (WT) and $Ghr^{-/-}$ mice. These animals were maintained in standard light conditions (12-hour light/dark cycle) and received filtered water and regular rodent chow ad libitum. The experiments were approved by the Ethics Committee on the Use of Animals of the Institute of Biomedical Sciences at the University of São Paulo and the Multidisciplinary Institute of Cell Biology (IMBICE).

Evaluation of GH- or Prolactin-responsive Neurons

To visualize GH-responsive cells in the mouse brain, ad libitum-fed adult mice received an IP injection of GH extracted from porcine pituitary (pGH; 20 µg/g body weight; National Hormone and Peptide Program, Torrance, CA) and were perfused at different time points (5, 10, 20, 30, 45, 60, and 90 minutes after injection). A similar approach was used to visualize human GH (hGH) or prolactin-responsive cells, except that recombinant hGH (20 µg/g body weight; Dong-A Pharmaceutical Co., Dalsung-Kun, Republic of Korea) or ovine prolactin (5 µg/g body weight; National Hormone and Peptide Program) was injected in mice that were perfused after 90 minutes. Another group of mice was cannulated in the lateral ventricle (P1Technologies, Roanoke, VA). After approximately 3 days of recovery, the animals received an intracerebroventricular (ICV) infusion of 2 µL of saline or pGH (3.33 µg/µL) and were perfused after different time points (5, 10, and 30 minutes after ICV injection). Mice were anesthetized with isoflurane and perfused with saline, followed by a 10% buffered formalin solution. Brains were collected and postfixed in the same fixative for approximately 1 hour and cryoprotected overnight at 4 °C in 0.1 M PBS containing 20% sucrose. Brains were cut into 30-µm-thick sections using a freezing microtome.

Immunofluorescence Reactions

Brain slices were rinsed in 0.02 M potassium PBS, pH 7.4 (KPBS), followed by pretreatment in a water solution containing 1% hydrogen peroxide and 1% sodium hydroxide for 20 minutes. Then, sections were rinsed in KPBS, incubated in 0.3% glycine and 0.03% lauryl sulfate for 10 minutes each, and blocked in 3% normal goat serum for 1 hour, followed by incubation in a rabbit anti-$pSTAT5^{Tyr694}$ antibody (1:1000; Cat# 9351; RRID: AB_2315225; Cell Signaling Technology, Danvers, MA, USA) for 2 days. In double immunofluorescence reactions, brain series were also incubated in a mouse anti-vimentin antibody (1:200; Cat# sc-373717; RRID: AB_10917747; Santa Cruz Biotechnology, Inc.). Subsequently, sections were rinsed in KPBS and incubated

for 90 minutes in Alexa Fluor-conjugated secondary antibodies (1:500, RRID: AB_2576217 and AB_2340846; Jackson ImmunoResearch, West Grove, PA). Sections were mounted onto gelatin-coated slides and covered with Fluoromount G mounting medium (Electron Microscopic Sciences, Hatfield, PA). Photomicrographs were acquired with a Zeiss Axiocam 512 color camera adapted to a Zeiss Axioimager A1 microscope (Zeiss, Munich, Germany).

Immunoperoxidase Reaction

Immunoperoxidase staining against pSTAT5 was carried out as described for the immunofluorescence reactions, except that brain sections were incubated for 1 hour in a biotin-conjugated donkey anti-rabbit secondary antibody (1:1000, RRID: AB_2315225; Jackson ImmunoResearch), followed by a 1-hour incubation in an avidin-biotin complex (1:500, Vector Laboratories, Burlingame, CA). After thorough rinsing in KPBS, the peroxidase reaction was performed using 0.05% 3,3′-diaminobenzidine and 0.03% hydrogen peroxide. Finally, sections were rinsed in KPBS, mounted on gelatin-coated slides, dehydrated through ascending ethanol concentrations, transferred into xylene, and covered with DPX mounting medium (Sigma, St. Louis, MO).

In Situ Hybridization

Free-floating brain sections of hGH-injected mice (90 minutes after an IP injection; 20 µg/g body weight) were subjected to in situ hybridization using *Ghr*^{35}S- and *Prlr*^{35}S-labeled riboprobes. The detailed protocol and the sequence recognized by the radiolabeled probes are described in our previous publication (24). Subsequently, immunoperoxidase reaction was used in these tissues to label pSTAT5 immunoreactive cells.

Analysis of the *Ghr* and *Prlr* mRNA In Situ Hybridization Histochemistry Datasets From the Allen Institute Collection

The distribution of neurons expressing *Ghr* and *Prlr* mRNA was assessed by the analysis of the coronal in situ hybridization histochemistry datasets available at http://mouse.brain-map.org/experiment/show/14376 and http://mouse.brain-map.org/experiment/show/18879, respectively, from the Allen Institute collection (37). Images correspond to 25-µm sagittal brain sections that were 100 µm apart.

Analysis of *Ghr* and *Prlr* Expression Using Single Cell Transcriptomic Datasets

The expression of *Ghr* in different hypothalamic cell types was assessed using a publicly available combined whole hypothalamus scRNA-sequencing dataset (38), which compiles 18 previously published datasets. We identified all cells positive for the *Ghr* and *Prlr* genes, defined as those having 1 or more counts for each corresponding gene in the raw counts matrix, and using the accompanying metadata, we analyzed the frequency of *Ghr*- and *Prlr*-expressing cells within the clusters assigned to tanycytes and endothelial cells. Processing of the database was performed in R 4.3.2/Rstudio 421. Original data can be accessed at https://doi.org/10.17863/CAM.87955.

Hormone Assessment

To determine the impact of a systemic pGH injection on blood GH levels in a dose sufficient to induce robust phosphorylation of STAT5 in the mouse brain (24), blood samples of C57BL/6J mice were collected at baseline and 5, 10, 15, 20, 30, 45, 60, 90, and 120 minutes after an IP pGH injection either at a dose of 5 or 20 µg/g of body weight. The control group received a saline injection. To collect CSF, anesthetized WT mice were placed in a stereotaxic frame with their head forming a 135-degree angle with respect to the body and IP injected with saline alone or containing ghrelin (0.2 µg/g of body weight) or pGH (5 or 20 µg/g of body weight). The results of both pGH doses were combined. At 20 minutes after treatment, ~10 µL of CSF was collected from the cisterna magna, as described in detail elsewhere (18). CSF samples were immediately frozen on dry ice and later stored at −80 C. Then, anesthetized mice were decapitated, and blood samples were collected in tubes pretreated with EDTA (1 mg/mL final). Blood samples were centrifuged, and plasma was incubated at 37 °C for 30 minutes and then kept at 4 °C for 1 hour. Finally, serum was separated by centrifugation at 5000 rpm for 5 minutes at 4 °C and stored at −80 °C until processing. GH concentrations were assessed using an in-house enzyme-linked immunosorbent assay (32, 39-42). Our previous experiments showed that the lower limit of detection and the intra-assay and interassay coefficients of variation were 0.04 ng/mL, 2.6%, and 9.7%, respectively.

Transport of Radiolabeled GH to the Hypothalamus

Ghr$^{-/-}$ and control WT mice were used in this experiment. pGH (5 µg) was radioactively labeled with 3.7 MBq of ^{131}I by the chloramine T method and used immediately after preparation. Stability and radiochemical purity were evaluated as previously described (43, 44). Briefly, we obtained high radiochemical purity with a radiolabeling yield greater than 95%. Furthermore, the radiolabeling, diluted in fetal bovine serum, remained stable for at least 13 hours. To determine whether radioactively iodinated pGH (^{131}I-pGH) can permeate the hypothalamus without a functional *Ghr* gene, an IP injection of 0.1 mL saline solution containing 10^6 cpm of ^{131}I-pGH was administered to *Ghr*$^{-/-}$ mice. At time points ranging from 2 to 25 minutes after injection, mice were euthanized, blood was collected via the aorta, the brain removed, and the hypothalamus separated. Two animals were used for each time point. WT animals received twice the injected dose as a control because they were twice the average size and weight of *Ghr*$^{-/-}$ mice. Hypothalamic tissue was weighed, and radiation levels were counted in the hypothalamus and 75 µL of blood using a Gamma counter (PerkinElmer 2470 Wizard Automatic Gamma Counter; PerkinElmer Life and Analytical Sciences, Waltham, MA). The percentage of injected dose per gram of tissue was calculated based on the injected activity and the activity detected in the tissue. The tissue/blood ratio was given by dividing tissue activity by blood activity.

Single-photon Emission Computed Tomography

This study used recombinant mouse GH (mGH) synthesized at the Biotechnology Center of the IPEN-CNEN/SP. An IP injection of saline containing ^{123}I-mGH with an activity of 37 MBq was injected in male WT mice. Mice were euthanized by decapitation using a guillotine at 2 and 10 minutes after the injection. Their heads were placed in the scanning chamber, and images were obtained for 1 hour. The location of the hormone in the anatomical regions of the brain was assessed using single-photon emission computed tomography (SPECT-CT),

analyzed on microPET Albira (Bruker Biospin Corporation, Woodbridge, CT, USA) with the following protocols: 3D FOV80 PH 30 seg/prog for SPECT and Good 35 Kev 400 µA for CT. The images were processed using PMOD software (PMOD Technologies, Zurick, Switzerland) in partnership with the IPEN Radiopharmacy Center.

Statistical Analysis

Statistical analyses were performed using the Prism software (GraphPad, San Diego, CA). Two-way repeated measures ANOVA, 1-way ANOVA, and regular linear regression were used according to each experiment. The statistical tests used are described in the figure legends. All results are expressed as mean ± standard error of the mean.

Results

Systemically Injected GH Rapidly Induces pSTAT5 in ARH Neurons Near the ME

We initially determined the effects of supraphysiological GH injections on blood GH levels. Both 5 and 20 µg/g body weight doses induced robust increases in blood GH levels compared to saline-injected mice (Fig. 1A). The 20 µg/g body weight dose caused higher blood GH levels than the 5 µg/g body weight dose. Blood GH levels remained high throughout the 120-minute analysis period (Fig. 1A). Of note, the increase in blood GH levels was already detected 5 minutes after injection (Fig. 1A). Thus, the dose of GH used in the current study causes rapid and sustained elevations in blood GH levels of mice.

We decided to use the 20 µg/g body weight dose in the following experiments, similar to that used in our previous studies to detect GH-responsive cells via STAT5 phosphorylation (24, 31, 41, 45). In the next experiment, the pattern of pSTAT5 immunoreactive cells was analyzed over time in the brains of mice that received an IP pGH injection. Very few pSTAT5 immunoreactive cells were detected in the brain 5 minutes after an IP injection of pGH (Figs. 1B-1G and 2A-2C), in accordance with the pattern observed in saline-injected mice (24, 26). The exception was a weak but evident pSTAT5 staining observed in the ARH of mice perfused 5 minutes after pGH injection (Figs. 1B and 3A). The pSTAT5 staining was limited to the ventromedial part of the ARH (Fig. 3A). Furthermore, pSTAT5 immunoreactivity was not restricted to the cell nucleus, as usual, but appears to be a cytoplasmic staining (Fig. 3A). Cytoplasmic staining indicates that STAT5 was recently phosphorylated and has not yet been translocated to the nucleus. Thus, ARH neurons near the ME are the first to detect a systemic GH injection.

GH-induced pSTAT5 in the Hypothalamic Parenchyma Showed a Medial-to-lateral Pattern Over Time

Brain pSTAT5 immunoreactivity in response to a systemic pGH injection was analyzed over time (Fig. 1B-1G). GH-induced pSTAT5 immunoreactive cells were detected in the periventricular nucleus (PV; Figs. 2D and 4A), and the entire extension of the ARH (Figs. 2E and 3B) of mice perfused 10 minutes after pGH injection. After 20 minutes postinjection, pGH-induced pSTAT5 immunoreactive cells were detected in the paraventricular nucleus of the hypothalamus (PVH; Figs. 2G and 4B), in neurons of the ventromedial nucleus of the hypothalamus (VMH) that are closest to the ARH (Figs. 2H and 3C) and in the most medial portion of the dorsomedial nucleus of the hypothalamus (DMH; Fig. 2I). Noteworthy, although the pSTAT5 immunoreactivity in most medial PVH cells is nuclear, a weak and cytoplasmatic pSTAT5 staining was observed in the lateral PVH cells in mice perfused after 20 minutes of IP pGH injection (Fig. 4B). This difference suggests that STAT5 phosphorylation is at different time stages throughout PVH neurons. Thirty minutes after pGH injection, pSTAT5 immunoreactivity was observed in the entire PVH (Figs. 2J and 4C) and ARH (Figs. 2K and 3D) and approximately half of the VMH (portion close to the ARH; Figs. 2K and 3D) and DMH (portion close to the third ventricle; Fig. 2L). Notably, some brain areas near the lateral or fourth ventricles, such as the bed nucleus of the stria terminalis, anterior paraventricular nucleus of the thalamus, posterior hypothalamic area, and periaqueductal gray and Locus Coeruleus, express the *Ghr* mRNA and exhibit GH-induced pSTAT5 (24, 39, 46, 47). However, these nuclei showed small numbers of GH-induced pSTAT5 positive cells in shorter periods between the IP GH injection and perfusion (5-30-minute time window). GH-induced pSTAT5 immunoreactivity was observed in all brain nuclei 45 minutes postinjection when it affected not only the previously listed brain areas but also the entire hypothalamus (Figs. 2M-2O and 4D), amygdala, hippocampus, and brainstem (data not shown). Thus, brain areas near the lateral or fourth ventricles require significantly more time to express GH-induced pSTAT5 after an IP injection compared to nuclei located near the third ventricle. Minor differences in pGH-induced pSTAT5 staining were observed when comparing animals perfused after 45, 60, and 90 minutes postinjection (data not shown). These findings indicate that blood-derived GH acts differentially on the mouse brain, exhibiting a very specific and dynamic pattern.

To investigate if systemically injected pGH reaches the CSF, we analyzed GH concentration in the CSF collected from the cisterna magna 20 minutes after a systemic injection of ghrelin, pGH, or vehicle. We confirmed that both ghrelin (8.77 ± 3.31 ng/mL) and pGH injections (16.14 ± 5.19 ng/mL) increased serum GH levels compared to vehicle-injected mice (2.46 ± 1.51 ng/mL). However, CSF GH concentrations were below the detection limit in all experimental groups. Thus, increments in plasma GH concentration, induced by either exogenous administration of GH or the release of endogenous GH, do not acutely affect GH levels in the mouse CSF, at least after 20 minutes.

GH Can Rapidly Induce pSTAT5 in Cells Near Other CVOs

The action of blood-derived GH from other CVOs was analyzed. A weak and cytoplasmatic pSTAT5 staining was observed near the OVLT of mice 5 minutes after IP pGH injection (Fig. 5A). Conversely, no pSTAT5 immunoreactivity was observed in the AP and nucleus tractus solitarii (NTS) at this time (Fig. 5B). At 10 minutes after pGH injection, numerous pSTAT5 immunoreactive cells were detected near the OVLT (Fig. 5C). In addition, pSTAT5 immunoreactive cells were detected in the AP and part of the NTS adjacent to the AP (Fig. 5D). At 20 minutes postinjection, pGH-induced pSTAT5 immunoreactive cells were broadly distributed in

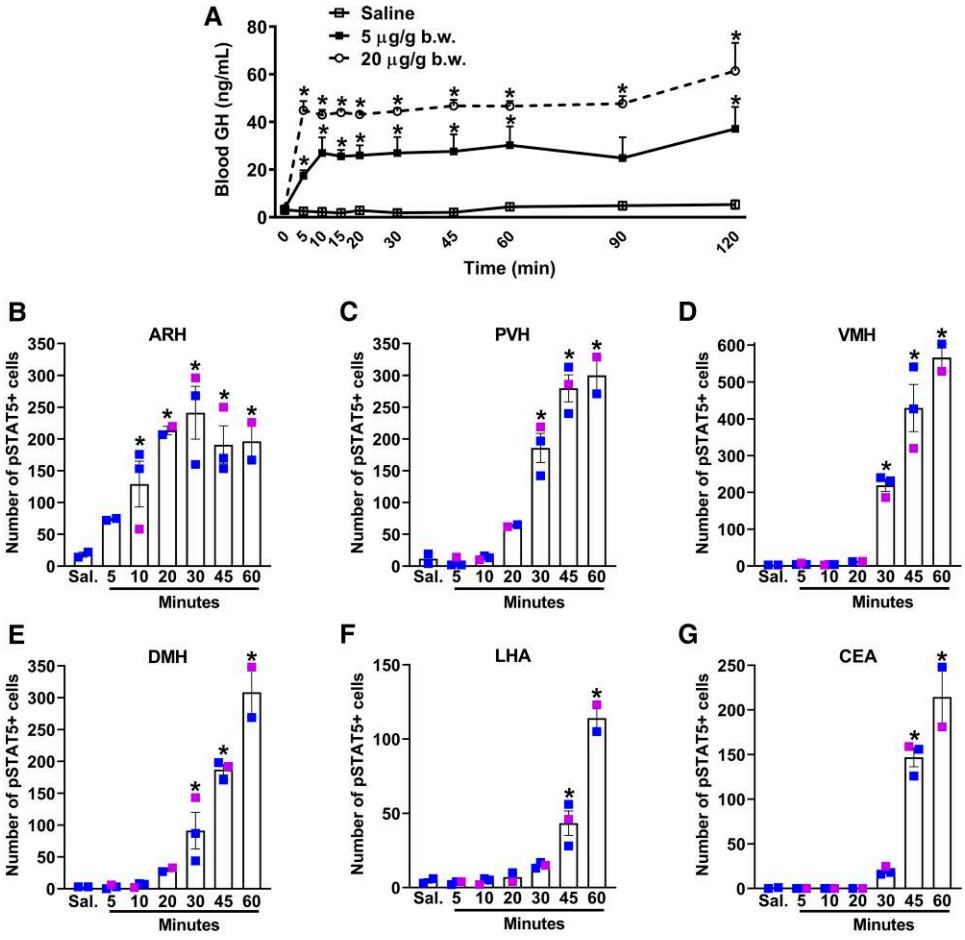

Figure 1. Blood GH levels and number of pSTAT5-positive cells in the brain of C57BL/6J mice after IP injections of saline or pGH. (A) Blood GH levels in male C57BL/6J mice after an IP injection of saline or pGH (n = 4/group). (B-G) Quantification of pSTAT5-positive cells in different brain nuclei and time points of male (blue symbol) and female (pink symbol) C57BL/6J mice after IP injections of sal. (saline) or pGH (n = 2-3/group). The time on the X-axis refers to the minutes spent after the pGH injection until perfusion. *$P < .05$ vs saline. Repeated measures 2-way ANOVA (A) or 1-way ANOVA (B-G).

areas neighboring the OVLT (Fig. 5E) and NTS (Fig. 5F). Thirty minutes after IP pGH injection, pSTAT5 immunoreactive cells could be found relatively far from the OVLT (Fig. 5G). Furthermore, neurons of the dorsal motor nucleus of the vagus nerve exhibited pSTAT5 immunoreactivity 30 minutes after IP pGH injection (Fig. 5H), in accordance with previous studies showing that the dorsal motor nucleus of the vagus nerve presents cholinergic GH-responsive neurons (26, 48). Thus, GH can rapidly induce pSTAT5 in cells near the OVLT and AP, although requiring a slightly longer time than observed in the ME.

Centrally Injected GH Induces a Medial-to-lateral Pattern of pSTAT5 Over Time

The following experiment evaluated the GH action pattern in the brain after an ICV injection (Fig. 6). Saline-injected mice exhibit only small numbers of pSTAT5 immunoreactive cells in the PV and ARH (Fig. 6A-6C), as previously described (26). The number of pSTAT5-immunoreactive cells in the PV and PVH increased 5 minutes after ICV pGH injection (Fig. 6D). The ARH exhibited a weak and cytoplasmic pSTAT5 staining 5 minutes after ICV pGH injection, which indicates early GH-induced GHR signaling (Fig. 6E and 6F). A robust increase in pSTAT5 immunoreactive cells was observed 10 minutes after ICV pGH injection in areas close to the third ventricle, including the PV, PVH (Fig. 6G), ARH (Fig. 6H), dorsomedial part of the VMH (Fig. 6H), and medial DMH (Fig. 6H). In contrast to systemically injected mice, an ICV pGH injection induced pSTAT5 in all brain nuclei known to express GHR that are near the brain ventricles, including the bed nucleus of the stria terminalis (Fig. 6J), medial and lateral septum (Fig. 6J), anterior paraventricular nucleus of the thalamus (Fig. 6K), and posterior hypothalamic area (Fig. 6L). Total responsiveness to an ICV pGH injection was observed after 30 minutes, where even more lateral areas showed GH-induced pSTAT5 immunoreactivity (Fig. 6J-6L). Thus, these findings provide evidence that centrally injected GH initially acts on brain areas near all ventricles, with a medial to lateral pattern, and then acts in more distant brain areas.

Ghr mRNA is Poorly Expressed in the Mouse Choroid Plexus

In the next series of experiments, we investigated whether the choroid plexus, an essential part of the blood-CSF barrier (49), is directly responsive to pGH. In contrast with the marked number of pGH-responsive cells in the hypothalamus, an acute

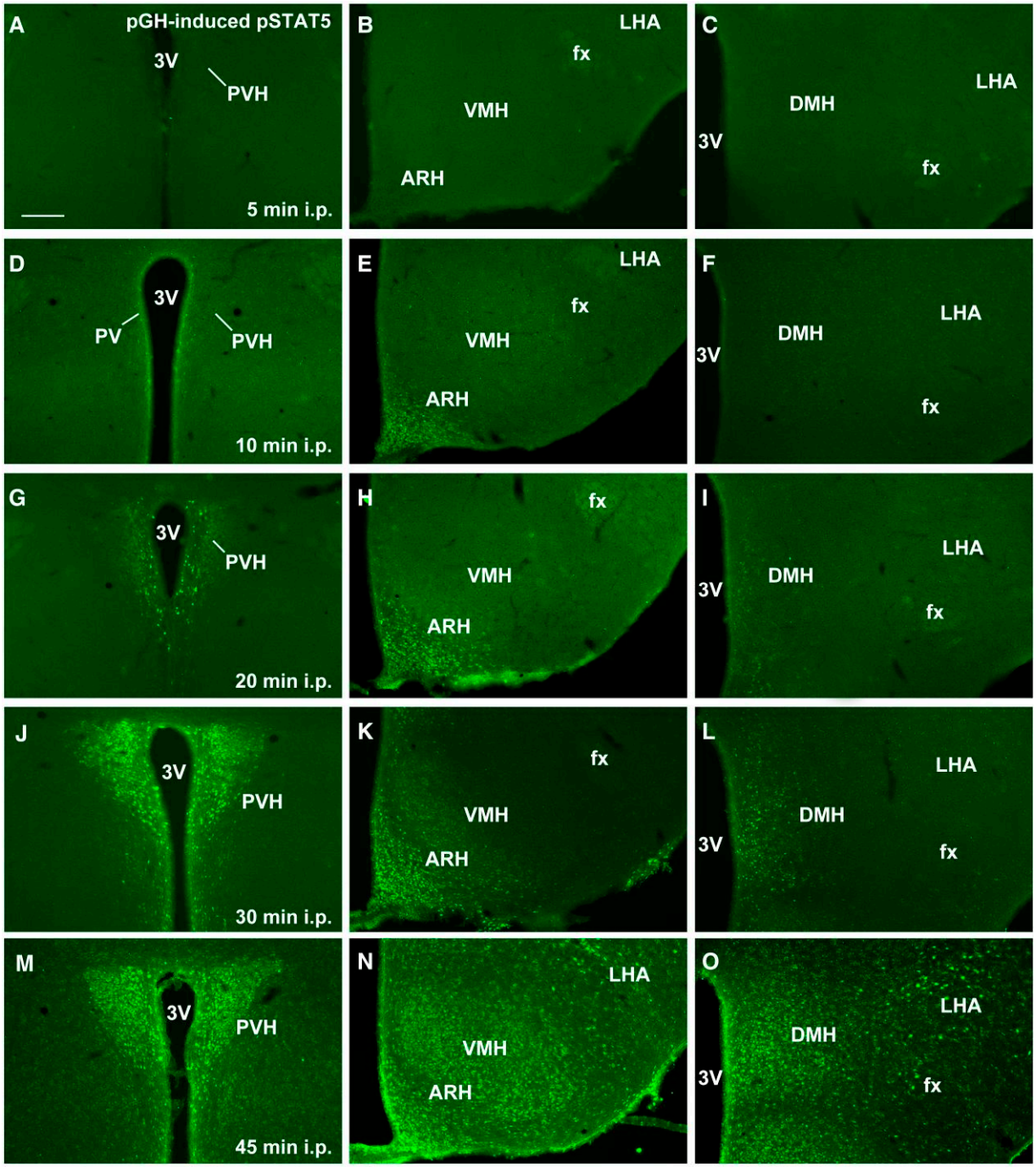

Figure 2. Immunoreactivity to pSTAT5 in the hypothalamus at different time points after an IP injection of pGH. (A-O) Fluorescence photomicrographs showing pSTAT5 immunoreactive cells in the hypothalamus of C57BL/6J mice that received an IP injection of pGH (20 µg/g body weight) and were perfused after 5 (A-C), 10 (D-F), 20 (G-I), 30 (J-L), and 45 minutes (M-O) postinjection (n = 2/group).

Abbreviations: 3V; third ventricle; ARH, arcuate nucleus of the hypothalamus; DMH, dorsomedial nucleus of the hypothalamus; fx, fornix; LHA, lateral hypothalamic area; PV, periventricular nucleus; PVH, paraventricular nucleus of the hypothalamus; VMH, ventromedial nucleus of the hypothalamus. Scale bar = 200 µm.

IP pGH injection induced only a few pSTAT5-immunoreactive cells in the choroid plexus, regardless of the time between injection and perfusion (Fig. 7A). Similar findings were observed after an ICV pGH injection (Fig. 7B). The weak pGH-induced pSTAT5 seems to be against previous studies showing that the choroid plexus is a strong binding site to hGH (23, 50). However, hGH, unlike mGH or pGH, activates not only GHR but also PrlR (51), which is expressed at much higher levels than GHR in the mouse choroid plexus (Fig. 7C and 7D). To clarify the apparent discrepancy between our observations using pGH and previous reports using hGH, we performed a simultaneous analysis of hGH-induced pSTAT5 (brown staining) and *Ghr* or *Prlr* mRNA (black silver grains; Fig. 7E and 7F). In contrast to the results observed after an IP injection of

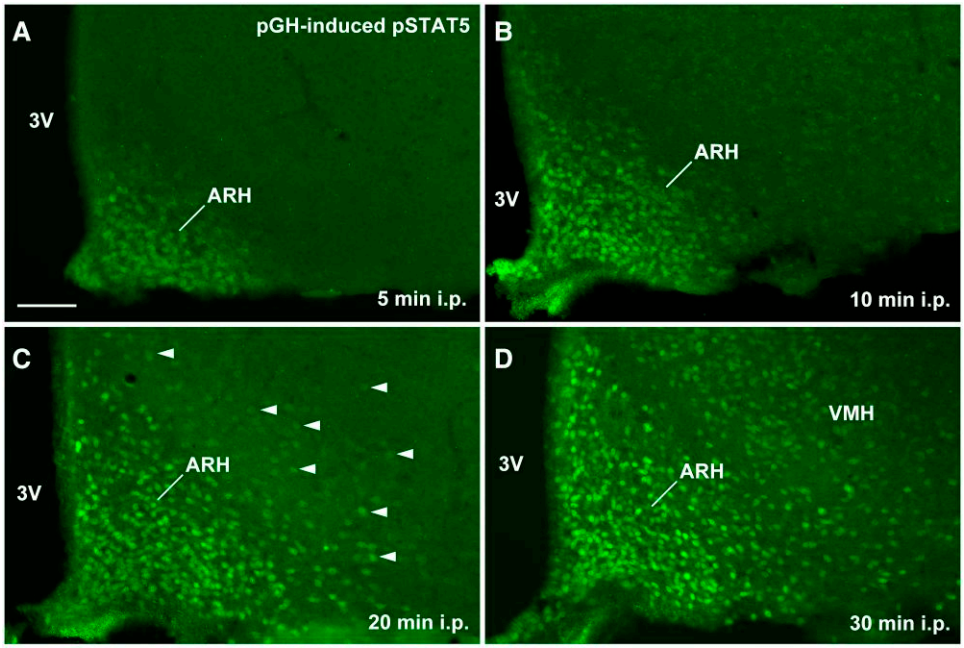

Figure 3. Immunoreactivity to pSTAT5 in the arcuate nucleus of the hypothalamus at different time points after an IP injection of pGH. (A-D) Fluorescence photomicrographs showing pSTAT5 immunoreactive cells in the arcuate nucleus of the hypothalamus (ARH) of C57BL/6J mice that received an IP injection of pGH (20 µg/g body weight) and were perfused after 5 (A), 10 (B), 20 (C), and 30 minutes (D) postinjection (n = 2/group). The arrowheads indicate the appearance of the first GH-responsive cells in the ventromedial nucleus of the hypothalamus (VMH). Note that these cells are close to the ARH, suggesting that pGH diffused from the ARH to the VMH.

Abbreviation: 3V; third ventricle. Scale bar = 100 µm.

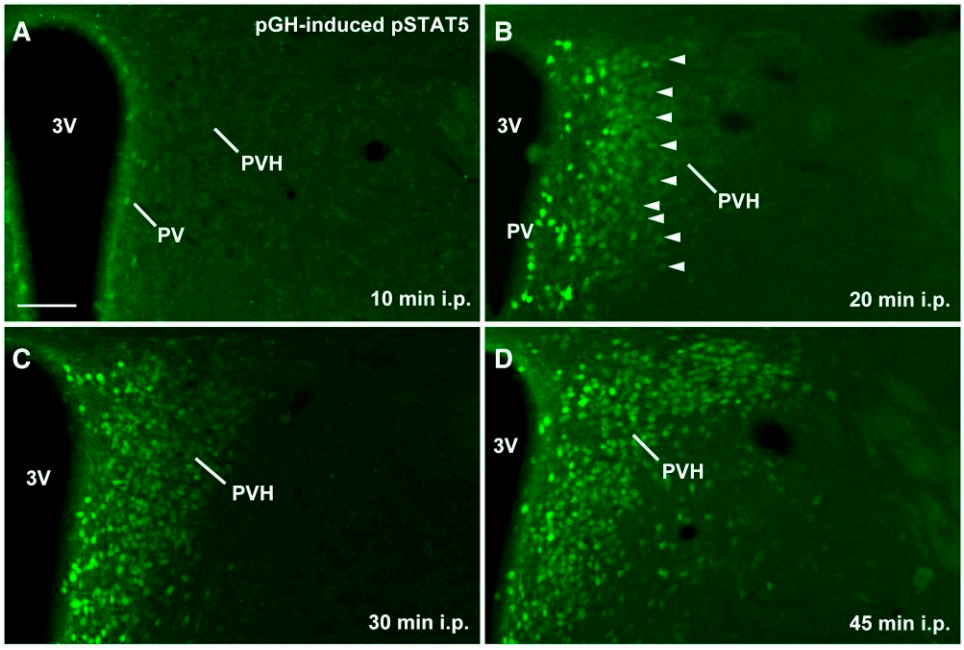

Figure 4. Immunoreactivity to pSTAT5 in the paraventricular nucleus of the hypothalamus at different time points after an IP injection of pGH. (A-D) Fluorescence photomicrographs showing pSTAT5 immunoreactive cells in the paraventricular nucleus of the hypothalamus (PVH) of C57BL/6J mice that received an IP injection of pGH (20 µg/g body weight) and were perfused after 10 (A), 20 (B), 30 (C), and 45 minutes (D) postinjection (n = 2/group). The arrowheads indicate a weak and cytoplasmatic pSTAT5 staining in cells of the lateral PVH. This staining differs from the robust and nuclear pattern typically observed in GH-responsive cells (see this typical pattern in the cells of the periventricular nucleus [PV]).

Abbreviation: 3V; third ventricle. Scale bar = 100 µm.

pGH, hGH induced pSTAT5 in many choroid plexus cells (Fig. 7E and 7F). Furthermore, although *Ghr* mRNA was weakly labeled in the choroid plexus (Fig. 7E), a robust *Prlr* mRNA expression was detected (Fig. 7F). Finally, we confirmed that an IP injection of prolactin induced a robust pSTAT5 staining in the mouse choroid plexus (Fig. 7G). Thus, these findings indicate that *Ghr* mRNA is poorly expressed in the mouse choroid plexus.

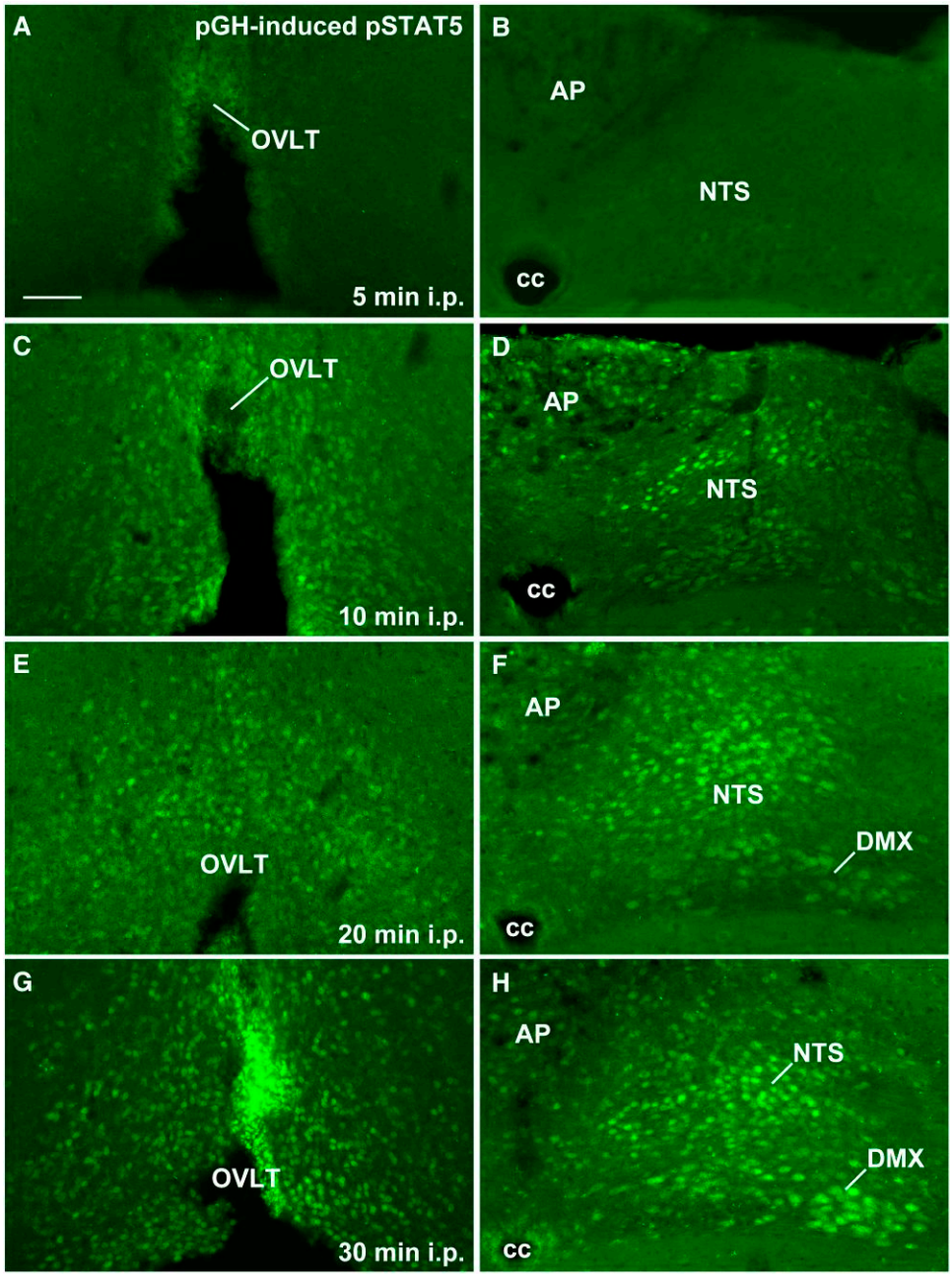

Figure 5. GH can rapidly diffuse through other circumventricular organs besides the median eminence. (A-H) Fluorescence photomicrographs showing pSTAT5 immunoreactive cells near the organum vasculosum of the lamina terminalis (OVLT) and in the caudal solitary complex (near the area postrema [AP]) of C57BL/6J mice that received an IP injection of pGH (20 µg/g body weight) and were perfused after 5 (A-B), 10 (C-D), 20 (E-F), and 30 minutes (G-H) postinjection (n = 2/group).

Abbreviations: cc, central canal; DMX, dorsal motor nucleus of the vagus nerve; NTS, nucleus tractus solitarii. Scale bar = 100 µm.

GH Transport Into the Mouse Brain is GHR-independent and Preferentially Occurs in the Hypothalamus

Next, we determined the kinetics of brain accessibility of GH by analyzing blood and brain radioactivity in mice systemically injected with ^{131}I-pGH. The transport of ^{131}I-pGH into the hypothalamus was compared between WT and *Ghr*$^{-/-}$ mice (Fig. 8). The slope in the WT mice was significantly different from zero ($F_{(1,6)} = 13.37$, $P = .0106$), whereas a tendency was observed in *Ghr*$^{-/-}$ mice ($F_{(1,6)} = 5.113$, $P = .0644$; Fig. 8). However, no difference in the slope was observed between the groups ($P = .7345$). Thus, GH is transported into the mouse brain, and its transport is independent of functional GHR.

We used SPECT-CT to gain neuroanatomical insights into brain areas reached by the systemically injected radioactive GH. We confirmed that 2 minutes after an IP injection, ^{123}I-mGH was predominantly detected in the ventral surface of the tuberal hypothalamus, where the ARH and ME are located (Fig. 9). The detection intensity increased 10 minutes after the ^{123}I-mGH injection. Still, the most significant activity remained concentrated in the ventral surface of the hypothalamus (Fig. 9), which agrees with the temporal evolution of pGH-induced pSTAT5 labeling (Fig. 2).

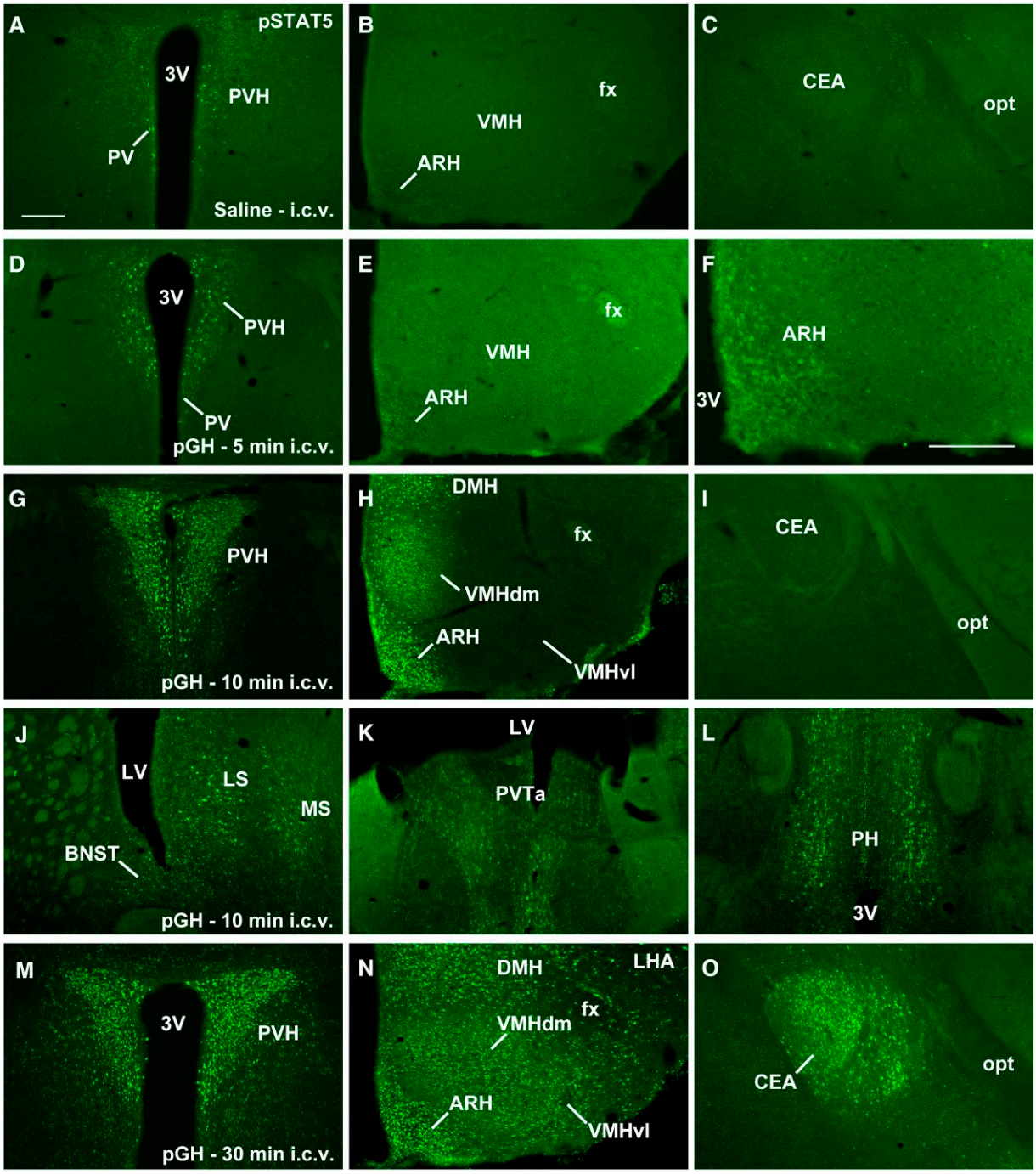

Figure 6. GH diffuses from the cerebrospinal fluid to the brain parenchyma. (A-O) Fluorescence photomicrographs showing pSTAT5 immunoreactive cells in the hypothalamus and amygdala of C57BL/6J mice that received an ICV injection of saline (2 µL; A-C) or pGH (6.66 µg in 2 µL) and were perfused after 5 (D-F), 10 (G-L), and 30 minutes (M-O) postinjection (n = 2-4/group).

Abbreviations: 3V; third ventricle; ARH, arcuate nucleus of the hypothalamus; BNST, bed nucleus of the stria terminalis; CEA, central nucleus of the amygdala; DMH, dorsomedial nucleus of the hypothalamus; fx, fornix; LHA, lateral hypothalamic area; LS, lateral septum; LV, lateral ventricle; MS, medial septum; opt, optic tract; PH, posterior hypothalamic area; PV, periventricular nucleus; PVH, paraventricular nucleus of the hypothalamus; PVTa, anterior paraventricular nucleus of the thalamus; VMH, ventromedial nucleus of the hypothalamus; VMHdm, dorsomedial part of the VMH; VMHvl, ventrolateral part of the VMH. Scale bars = 200 µm.

GH Can Target a Subset of Hypothalamic Tanycytes

Overall, circulating GH seems to differentially target brain areas near the CVOs. Because tanycytes are a characteristic feature of all CVOs regulating the exchange between the blood and the brain (52), we tested the hypothesis that tanycytes could enhance GH's action. Here, we focused on the hypothalamic tanycytes, one of the most well-characterized types of ependymal cells (3). The analysis of the transcriptome data produced by Steuernagel et al (38) revealed that 676 hypothalamic tanycytes (6.9% of all hypothalamic tanycytes) contained at least 1 count for *Ghr* mRNA (Fig. 10A). Interestingly, at least 1 count for *Ghr* mRNA was also detected in 1006 brain endothelial cells (9.8% of total brain endothelial cells; Fig. 10A). Conversely, only 168

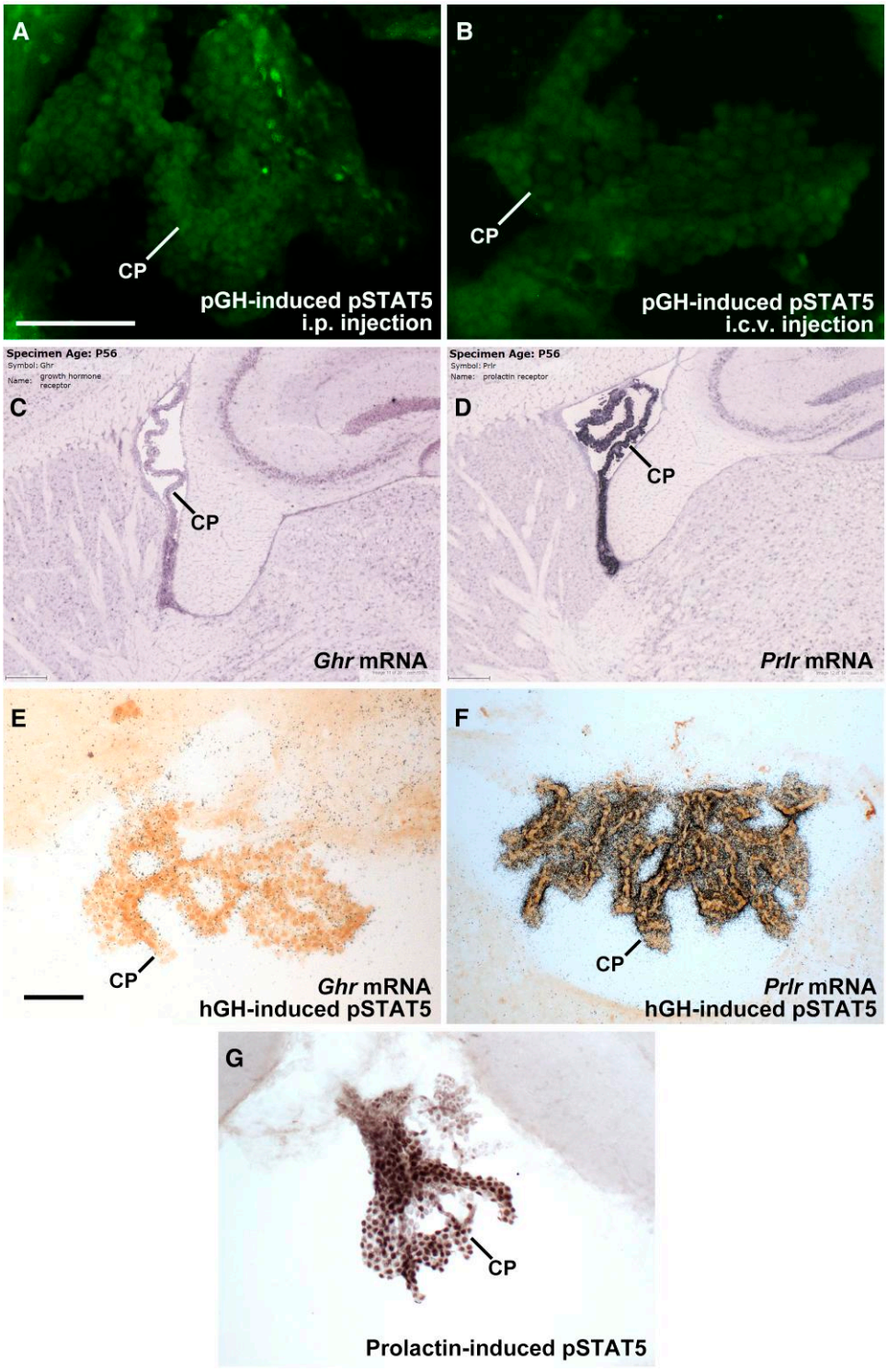

Figure 7. *Ghr* mRNA is poorly expressed in the mouse choroid plexus. (A) Choroid plexus exhibits very few pSTAT5 immunoreactive cells after an IP pGH injection. (B) Choroid plexus exhibits very few pSTAT5 immunoreactive cells after an ICV pGH injection. (C, D) In situ hybridization photomicrographs from the Allen Brain Atlas show poor *Ghr* mRNA expression in the mouse choroid plexus (C), whereas *Prlr* mRNA is highly expressed (D). (E) Co-localization between hGH-induced pSTAT5 (brown staining) and *Ghr* mRNA (black silver grains) in the mouse plexus choroid. (F) Colocalization between hGH-induced pSTAT5 (brown staining) and *Prlr* mRNA (black silver grains) in the mouse plexus choroid. (G) An IP prolactin injection induces a robust pSTAT5 expression in the mouse choroid plexus.

Abbreviation: CP, choroid plexus. Scale bars = 100 µm.

hypothalamic tanycytes and 175 brain endothelial cells contained at least 1 count for *Prlr* mRNA, representing ~1.7% of each cell type (data not shown). Hypothalamic tanycytes are diverse and located at the level of the ME (β tanycytes), ARH (α2 tanycytes), and, more dorsally, at the VMH/DMH level (α1 tanycytes; Fig. 10B). The differential analysis of the previously referenced scRNA-seq dataset of the hypothalamic cells indicates that 417 and 259 β and α tanycytes contain at

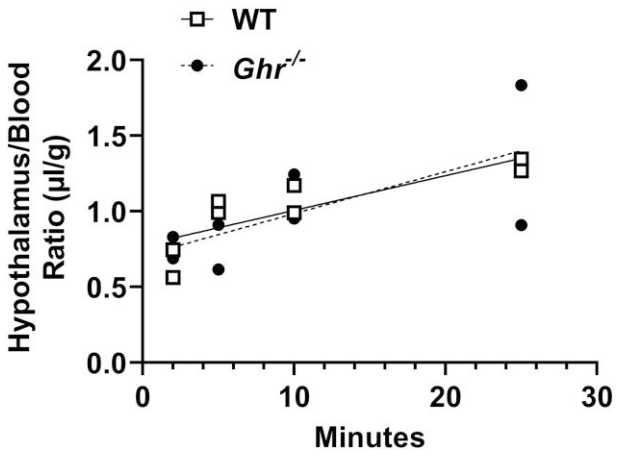

Figure 8. GH transport into the mouse brain is independent of functional GHR. Comparison between the transport of ^{131}I-pGH into the hypothalamus of wild-type (WT) and dwarf *Ghr* knockout (*Ghr*$^{-/-}$) mice. The slopes were calculated and compared by simple linear regression.

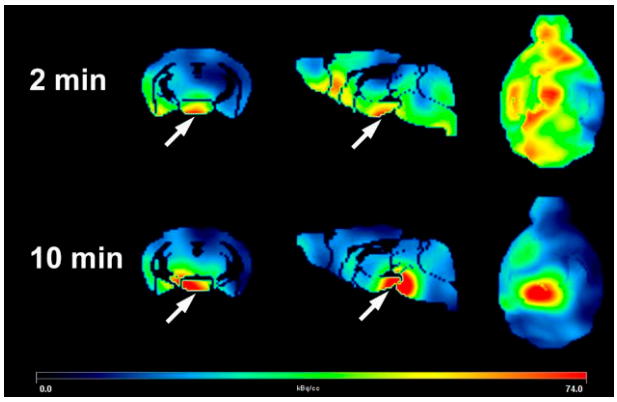

Figure 9. Diffusion of radiolabeled GH into the mouse brain using single-photon emission computed tomography (SPECT-CT). The images were obtained in mice that were euthanized 2 and 10 minutes after a systemic ^{123}I-mGH injection. The images show coronal, sagittal, and superior views of the brain. The arrows indicate the hypothalamus.

least 1 count for *Ghr* mRNA, representing 9.4% and 4.9% of each tanycyte cell type, respectively. To further assess the precise tanycyte subtypes responsive to GH, we assessed pGH-induced pSTAT5 using vimentin as a well-established marker of tanycytes (3). Numerous pGH-induced pSTAT5-positive cells lining the third ventricle floor at the ME level were observed, including tanycytes (Fig. 10C and 10D). Furthermore, an intense pGH-induced pSTAT5 staining was observed in the external layer of the ME, near vimentin-positive fibers, resembling numerous neuroendocrine terminals (insight 1 of Fig. 10D). pGH-induced pSTAT5 was virtually absent in vimentin-positive cells at the ARH and VMH/DMH levels, respectively (Fig. 10E and 10F). In contrast to pGH, prolactin produced only a moderate number of pSTAT5-positive cells on the third ventricle floor (Fig. 10G). In addition, we performed in situ hybridization against *Ghr* mRNA in hGH-injected mice. We detected *Ghr* mRNA-positive cells lining the third ventricle's floor coexpressing GH-induced pSTAT5 staining (Fig. 10H). In contrast, *Prlr* mRNA is poorly expressed in cells lining the floor of the third ventricle (Fig. 10I). Thus, these results suggest that GH can directly target β tanycytes.

Discussion

Because of its molecular size (~22 kDa), circulating GH is not expected to pass through the tight junctions of vascular endothelial cells of the BBB. Previous studies have consistently shown that systemic GH treatment results in rapid and potent activation of GHR-expressing cells located in a variety of brain areas (24, 26, 31, 39, 45, 48). However, the mechanisms by which GH reaches its brain targets have remained uncertain. Here, we used a variety of experimental strategies to comprehensively demonstrate that plasma GH displays a particular pattern of action in the mouse brain, involving brain areas located near the CVOs and some hypothalamic nuclei close to the third ventricle. Additionally, we showed that GH can access the mouse brain in a GHR-independent manner and can directly target hypothalamic tanycytes.

In the current study, we provided evidence that the first brain cells to detect circulating GH were those very close to CVOs. A few minutes after IP GH injection, pSTAT5 was detected in cells close to the ME (ventromedial ARH neurons) and OVLT. The permeability of GH is in accordance with the characteristics of fenestrated vessels of the ME that allow the extravasation of molecules with approximately 20 kDa (4). Compared to other brain nuclei, the rapid response of ARH neurons to systemically injected hormones was previously demonstrated using leptin (53). Faouzi et al elegantly showed that a subpopulation of ARH neurons has direct access to the systemic circulation; these cells present leptin-induced pSTAT3 earlier than any other neuronal population (53). In addition, ARH neurons require a low-dose systemic injection of leptin to exhibit pSTAT3 (53). These differences only occur after systemic leptin injection, whereas ICV leptin administration produces similar responses in ARH and non-ARH neurons (53). Therefore, the fenestrated capillaries of CVOs, particularly the ME, are a relatively fast gateway for different hormones in the central nervous system.

Periventricular areas of the hypothalamus exhibited GH-induced pSTAT5 in the second place. After that (approximately 20-30 minutes after an IP injection or 5 to 10 minutes after an ICV injection), a progressive increase in GH-induced pSTAT5 cells was observed in lateral nuclei, which may suggest that GH diffuses through the hypothalamus parenchyma from medial to lateral. Noble et al (54) showed that one-third of melanin-concentrating hormone-producing neurons project to the cerebral ventricles and melanin-concentrating hormone regulates feeding behavior via CSF volume transmission. However, the possibility of GH diffusion in the brain parenchyma is challenged by the minimal penetrance of different fluorescent tracers in the brain parenchyma after an ICV infusion, which is limited to the periventricular area (55). For instance, fluorescent-labeled ghrelin (3.3 kDa) presents a minimal diffusion in the hypothalamus parenchyma, whose penetrance was approximately 130 µm from the third ventricle (56). However, using pSTAT5 as a marker of GH-responsive cells, the GH penetrance seems much higher. It is important to stress that we used a pharmacological dose of GH to induce pSTAT5. This dose maintained circulating GH levels high for more than 2 hours. Thus, the high dose used in the current study may have facilitated GH diffusion via nonphysiological mechanisms. However, similar to GH, systemic or central injections of other hormones that recruit STAT signaling pathways, such as

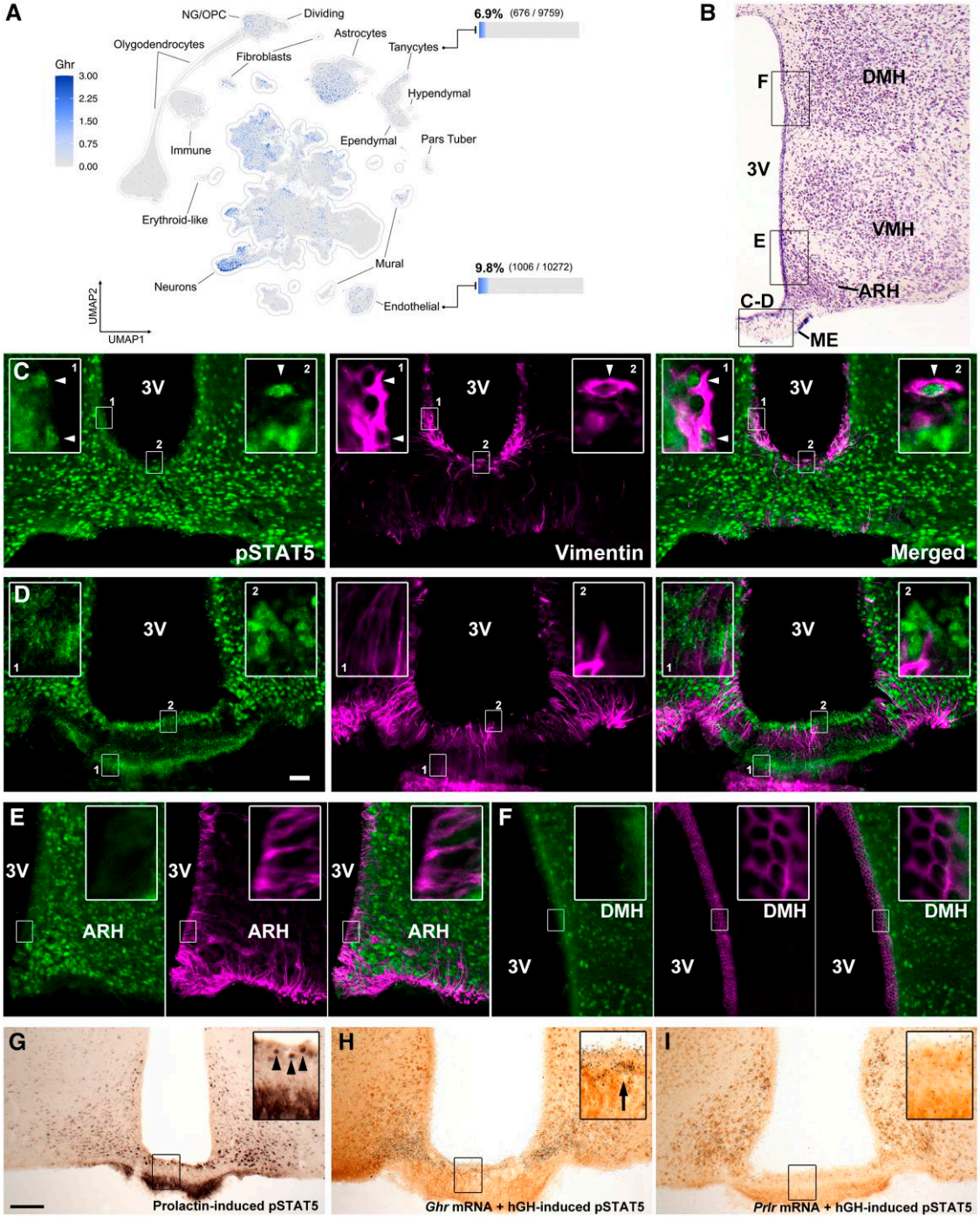

Figure 10. Tanycytes on the third ventricle floor are responsive to GH. (A) Uniform manifold approximation and projection (UMAP) plot showing the expression of *Ghr* mRNA in different mouse hypothalamic cell types. The location of major cell types is indicated with enclosing lines and labeled accordingly. For tanycytes and endothelial cells, the entire distribution of expression values is presented as a descending order stripe plot, along with the percentage of *Ghr*-positive cells as well as their absolute number for each population. Color corresponds to log-normalized expression values. (B) Representative Nissl's photomicrograph shows the different tanycyte cell populations analyzed. (C, D) Colocalization between pGH-induced pSTAT5 (green staining) and vimentin (magenta) in the cells layer on the third ventricle floor. Insights represent higher magnifications of the selected images. The arrowheads show double-labeled cells. (E, F) Colocalization between pGH-induced pSTAT5 (green staining) and vimentin (magenta) in different parts of the tuberal hypothalamus. (G) Prolactin-induced pSTAT5 on the third ventricle floor. Arrowheads indicate examples of prolactin-responsive cells. (H) Colocalization between hGH-induced pSTAT5 (brown staining) and *Ghr* mRNA (black silver grains) on the third ventricle floor/median eminence. The arrow indicates a strong *Ghr* mRNA expression. (I) Colocalization between hGH-induced pSTAT5 (brown staining) and *Prlr* mRNA (black silver grains) on the third ventricle floor/median eminence.

Abbreviations: 3V, third ventricle; ARH, arcuate nucleus; DMH, dorsomedial nucleus; ME, median eminence; VMH, ventromedial nucleus. Scale bars. D = 50 μm; E = 100 μm.

leptin or prolactin, are also able to reach cells far from the ventricles (eg, in the lateral hypothalamic area or amygdala) in a similar timeframe to GH (7, 24, 57-59). Whether these hormones reach those cells by volume transmission or other transport mechanisms is unknown. It is important to stress that we evaluated GH responsiveness only in basal

physiological conditions. GH secretion increases after different metabolic challenges, such as chronic food restriction, hypoglycemia, prolonged exercise, and pregnancy (60). Notably, the reduction of blood glucose levels during fasting induces alterations in the structural organization of the blood-hypothalamus barrier (61). Thus, future studies should explore whether metabolic challenges affect hypothalamic permeability to GH.

Several studies demonstrated an intense autoradiographic reaction in the choroid plexus induced by administration of radiolabeled hGH (23, 50, 62). The presence of GHR in the choroid plexus was suggested as a putative mechanism of transport of GH into the brain (50). Unlike mGH, pGH, or bovine GH, hGH is a lactogenic hormone that can bind both GHR and PrlR (51). In the current study, we observed a limited capacity of pGH in inducing pSTAT5 in choroid plexus cells. In addition, *Ghr* mRNA is poorly expressed in the mouse choroid plexus. In contrast, prolactin-induced pSTAT5 and *Prlr* mRNA are highly enriched in the mouse choroid plexus. Therefore, our findings suggest that the high binding capacity of radiolabeled hGH to the choroid plexus is explained by the hGH/PrlR interaction and not via GHR. However, Zhai et al (63). observed a high binding capacity of radiolabeled rat GH to the rat choroid plexus. It is currently unknown whether species differences exist in the expression of GHR between the choroid plexus of rats and mice. However, in accordance with our findings, administration of bovine GH does not compete with hGH to bind the choroid plexus but decreases the capacity of hGH to bind the hypothalamus (23, 62), suggesting that GHR is expressed in the hypothalamus and not in the choroid plexus. Our findings indicate that if the choroid plexus contributes to the GH transport into the brain, this participation seems mostly GHR independent.

Tanycytes represent another important cell population that forms the blood/CSF barrier (3, 13). Tanycytes in the ME have been recently investigated because of their role as a barrier to avoid the free diffusion of substances that pass through the fenestrated vessels to the CSF and hypothalamus (3, 13). Several studies demonstrated that β tanycytes are in direct contact with the vascular wall containing the fenestrated capillaries, so they can use hormone receptors to mediate the transport of proteins with a molecular weight similar to GH into the brain (14-17). Using transcriptome data available (38), we found that a subgroup of tanycytes, especially the β subtype, contained at least 1 count for *Ghr* mRNA, an observation further confirmed by in situ hybridization. It is worth noting that the fraction of tanycytes expressing *Ghr* mRNA may be underestimated in the transcriptomic analysis because of its low expression level, making it more susceptible to the so-called "drop-out" events, in which a gene is detected in some cells but not in others (64). Subsequently, we observed pGH-induced pSTAT5 mainly in β tanycytes. Notably, a high responsiveness to GH was observed in the third ventricle floor at the ME level. However, no further colocalization with vimentin was found at this level, probably because the soma of these β tanycytes is poorly labeled. Thus, additional colocalization studies are necessary to confirm whether these GH-responsive cells are mostly tanycytes. Interestingly, numerous pGH-induced pSTAT5 cells were also observed in the external layer of the ME. However, in this case, the staining appears to be neuroendocrine terminals, not cell nuclei, as observed in other areas. The external layer of the ME contains the nerve fibers of hypophysiotropic neurons that contact the fenestrated vessels to regulate the secretion of anterior pituitary hormones (65). Therefore, these numerous nerve terminals immunoreactive to pSTAT5 likely represent hypothalamic neuroendocrine neurons that produce dopamine, somatostatin, GH-releasing hormone, thyrotropin-releasing hormone, or corticotropin-releasing hormone and are responsive to GH, as previously shown (39, 40, 45, 66). It is tempting to hypothesize that GHR signaling may regulate these neuroendocrine terminals at the ME level. This possibility may represent a negative feedback mechanism using the fenestrated capillaries of the ME to control the somatotropic and other endocrine axes without GH having to cross the BBB or blood/CSF barrier. Further studies are necessary to investigate this possibility.

To investigate whether GH is transported in a blood-to-CSF direction, we assessed GH levels in the CSF from the cisterna magna of mice that were systemically treated with either GH or ghrelin, which induces the secretion of endogenous GH (1, 2, 32). The CSF in the cisterna magna serves as an indicator of the overall transport of molecules into the CSF because it receives fluid that has circulated throughout the entire ventricular system (67). Notably, we could not detect GH in the CSF of mice with robust elevations of GH concentrations in plasma. It is important to stress that CSF was collected 20 minutes after GH or ghrelin injections. So, it is unclear whether additional time is necessary to increase GH levels in the CSF. Nonetheless, this observation, together with the finding that cells of the choroid plexus lack *Ghr* expression or GH-induced pSTAT5, suggests that the choroid plexus is not the main player transporting GH into the brain. Conversely, the discovery that some β tanycytes express *Ghr* and respond to GH, coupled with the striking medial-to-lateral pattern of pSTAT5 induction in response to systemically injected GH, suggests that plasma GH may predominantly access the third ventricle and, consequently, the periventricular hypothalamic nuclei. The preferential access of systemic GH into the third ventricle, rather than other ventricles, is underscored by the observation that centrally administered GH induces pSTAT5 increments in brain areas expressing GHR but located near other brain ventricles, in contrast to systemic GH treatment.

Radiolabeled hormones have been extensively used to investigate the transport of hormones into the brain. Here, we compared the transport of radiolabeled GH into the hypothalamus between WT and $Ghr^{-/-}$ mice using a similar approach used to study prolactin transport into the mouse brain (21). Notably, a similar increase of radiolabeled GH was observed in the mouse hypothalamus over time comparing WT and $Ghr^{-/-}$ mice. Thus, this finding indicates that the rapid transport of GH into the mouse brain is GHR independent. This result is not surprising because, using other examples in the literature, *Prlr* knockout mice also show normal prolactin transport into the mouse brain (21). Of note, prolactin and GH, as well as their receptors, are homologous proteins and are thought to have arisen from common ancestral genes (68, 69). However, the striking difference in body weight and size between WT and $Ghr^{-/-}$ mice represents a confounding factor in this experiment. Although this difference was corrected by injecting different doses of radiolabeled GH for each group, it is unclear whether this approach affected our findings. Here, we also used SPECT-CT to gain neuroanatomical insights into the brain areas accessible to plasma GH. We found that radiolabeled mGH is detected just a few minutes after injection and mainly in the ventral surface of the

hypothalamus, where the ME and ARH are located. Despite our SPECT-CT study lacks the resolution to provide a detailed analysis of the distribution of radiolabeled GH, it confirmed that plasma GH has a preferential accessibility to the hypothalamic regions, as suggested by other studies reported here.

Important limitations and new questions raised by our study should be mentioned. Our observations indicate that the *Ghr* gene is not required to mediate the transport of GH into the brain. So, why do subgroups of tanycytes and brain endothelial cells express GHR? Second, the detection of GH action in the brain was only based on the ability of GHR to tyrosine phosphorylate STAT5 proteins. However, GHR can recruit different intracellular signaling pathways (22). Consequently, it is possible that a specific group of cells does not respond to GH by inducing pSTAT5, but rather alternative signaling pathways (70, 71). An example is leptin, in which the hippocampus expresses the leptin receptor. However, virtually no leptin-induced pSTAT3 is usually observed in this region (70, 71). Thus, the identification of additional markers of GH-responsive cells is desired. Finally, more than one mechanism may mediate the transport of GH into the brain but require different times. In this sense, brain endothelial cells, essential components of the BBB, express *Ghr* mRNA and may participate in the transport of GH into the brain, especially in areas that are distantly located from the CVOs or brain ventricles. However, this transport is likely slower than the other systems, potentially accounting for differences in time for GH to induce pSTAT5 between medial and lateral brain structures. Despite the lack of conclusive answers to these questions, the present study provides novel and valuable information about the pattern and mechanisms behind GH transport into the mouse brain.

Acknowledgments

We thank Ana Maria P. Campos for her technical assistance and Johana Miquet (IQUIFIB-CONICET, Argentina) for kindly providing the pGH for some experiments.

Funding

This work was supported by Fundação de Amparo à Pesquisa do Estado de São Paulo (FAPESP/Brazil; grants: 2016/20897-3 to F.W., 2020/10435-8 to C.R.J.S. and 2020/01318-8 to J.D.), Conselho Nacional de Desenvolvimento Científico e Tecnológico (CNPq/Brazil, 303363/2019-3 to J.D. and 305839/2021-7 to C.R.J.S.), and Fondo para la Investigación Científica y Tecnológica (FONCyT, PICT2017-3196, PICT2019-3054 and PICT2020-3270 to M.P.). J.J.K. was supported, in part, by the State of Ohio's Eminent Scholar Program that includes a gift from Milton and Lawrence Goll, National Institutes of Health grants NIH-R21AG081962, NIH-2R01AG059779, NIH-R01AR081804, NIH R25DK122952, the Edison Biotechnology Institute, and Diabetes Institute at Ohio University.

Disclosures

The authors have nothing to disclose.

Data Availability

The data supporting this study's findings are available from the corresponding author upon reasonable request.

References

1. Steyn FJ, Tolle V, Chen C, Epelbaum J. Neuroendocrine regulation of growth hormone secretion. *Compr Physiol*. 2016;6(2):687-735.
2. Murray PG, Higham CE, Clayton PE. 60 years of neuroendocrinology: the hypothalamo-GH axis: the past 60 years. *J Endocrinol*. 2015;226(2):T123-T140.
3. Prevot V, Nogueiras R, Schwaninger M. Chapter 16—tanycytes in the infundibular nucleus and median eminence and their role in the blood–brain barrier. In: Swaab DF Kreier F Lucassen PJ Salehi A and Buijs RM, eds. *Handbook of Clinical Neurology*. Elsevier; 2021:253-273.
4. Schaeffer M, Langlet F, Lafont C, *et al*. Rapid sensing of circulating ghrelin by hypothalamic appetite-modifying neurons. *Proc Natl Acad Sci U S A*. 2013;110(4):1512-1517.
5. Olofsson LE, Unger EK, Cheung CC, Xu AW. Modulation of AgRP-neuronal function by SOCS3 as an initiating event in diet-induced hypothalamic leptin resistance. *Proc Natl Acad Sci U S A*. 2013;110(8):E697-E706.
6. Chaves FM, Mansano NS, Frazao R, Donato J Jr. Tumor necrosis factor alpha and interleukin-1beta acutely inhibit AgRP neurons in the arcuate nucleus of the hypothalamus. *Int J Mol Sci*. 2020;21(23):8928.
7. Ramos-Lobo AM, Donato J Jr. The role of leptin in health and disease. *Temperature*. 2017;4(3):258-291.
8. Andermann ML, Lowell BB. Toward a wiring diagram understanding of appetite control. *Neuron*. 2017;95(4):757-778.
9. Hileman SM, Tornoe J, Flier JS, Bjorbaek C. Transcellular transport of leptin by the short leptin receptor isoform ObRa in madin-darby canine kidney cells. *Endocrinology*. 2000;141(6):1955-1961.
10. Hileman SM, Pierroz DD, Masuzaki H, *et al*. Characterizaton of short isoforms of the leptin receptor in rat cerebral microvessels and of brain uptake of leptin in mouse models of obesity. *Endocrinology*. 2002;143(3):775-783.
11. Li Z, Ceccarini G, Eisenstein M, Tan K, Friedman JM. Phenotypic effects of an induced mutation of the ObRa isoform of the leptin receptor. *Mol Metab*. 2013;2(4):364-375.
12. Nampoothiri S, Nogueiras R, Schwaninger M, Prevot V. Glial cells as integrators of peripheral and central signals in the regulation of energy homeostasis. *Nat Metab*. 2022;4(7):813-825.
13. Mullier A, Bouret SG, Prevot V, Dehouck B. Differential distribution of tight junction proteins suggests a role for tanycytes in blood-hypothalamus barrier regulation in the adult mouse brain. *J Comp Neurol*. 2010;518(7):943-962.
14. Balland E, Dam J, Langlet F, *et al*. Hypothalamic tanycytes are an ERK-gated conduit for leptin into the brain. *Cell Metab*. 2014;19(2):293-301.
15. Duquenne M, Folgueira C, Bourouh C, *et al*. Leptin brain entry via a tanycytic LepR-EGFR shuttle controls lipid metabolism and pancreas function. *Nat Metab*. 2021;3(8):1071-1090.
16. Kumar M P, Cremer AL, Klemm P, *et al*. Insulin signalling in tanycytes gates hypothalamic insulin uptake and regulation of AgRP neuron activity. *Nat Metab*. 2021;3(12):1662-1679.
17. Imbernon M, Saponaro C, Helms HCC, *et al*. Tanycytes control hypothalamic liraglutide uptake and its anti-obesity actions. *Cell Metab*. 2022;34(7):1054-1063e1057.
18. Uriarte M, De Francesco PN, Fernandez G, *et al*. Evidence supporting a role for the blood-cerebrospinal fluid barrier transporting circulating ghrelin into the brain. *Mol Neurobiol*. 2019;56(6):4120-4134.
19. Uriarte M, De Francesco PN, Fernandez G, *et al*. Circulating ghrelin crosses the blood-cerebrospinal fluid barrier via growth hormone secretagogue receptor dependent and independent mechanisms. *Mol Cell Endocrinol*. 2021;538:111449.
20. Rhea EM, Salameh TS, Gray S, Niu J, Banks WA, Tong J. Ghrelin transport across the blood-brain barrier can occur independently of the growth hormone secretagogue receptor. *Mol Metab*. 2018;18:88-96.

21. Brown RS, Wyatt AK, Herbison RE, *et al.* Prolactin transport into mouse brain is independent of prolactin receptor. *FASEB J*. 2016;30(2):1002-1010.
22. Dehkhoda F, Lee CMM, Medina J, Brooks AJ. The growth hormone receptor: mechanism of receptor activation, cell signaling, and physiological aspects. *Front Endocrinol (Lausanne)*. 2018;9:35.
23. Walsh RJ, Mangurian LP, Posner BI. The distribution of lactogen receptors in the mammalian hypothalamus: an in vitro autoradiographic analysis of the rabbit and rat. *Brain Res*. 1990;530(1):1-11.
24. Furigo IC, Metzger M, Teixeira PD, Soares CR, Donato J Jr. Distribution of growth hormone-responsive cells in the mouse brain. *Brain Struct Funct*. 2017;222(1):341-363.
25. Cady G, Landeryou T, Garratt M, *et al.* Hypothalamic growth hormone receptor (GHR) controls hepatic glucose production in nutrient-sensing leptin receptor (LepRb) expressing neurons. *Mol Metab*. 2017;6(5):393-405.
26. Wasinski F, Klein MO, Bittencourt JC, Metzger M, Donato J Jr. Distribution of growth hormone-responsive cells in the brain of rats and mice. *Brain Res*. 2021;1751:147189.
27. Donato J Jr, Wasinski F, Furigo IC, Metzger M, Frazao R. Central regulation of metabolism by growth hormone. *Cells*. 2021;10(1):129.
28. Campbell JN, Macosko EZ, Fenselau H, *et al.* A molecular census of arcuate hypothalamus and median eminence cell types. *Nat Neurosci*. 2017;20(3):484-496.
29. Chan Y, Steiner R, Clifton D. Regulation of hypothalamic neuropeptide-Y neurons by growth hormone in the rat. *Endocrinology*. 1996;137(4):1319-1325.
30. Kamegai J, Minami S, Sugihara H, Hasegawa O, Higuchi H, Wakabayashi I. Growth hormone receptor gene is expressed in neuropeptide Y neurons in hypothalamic arcuate nucleus of rats. *Endocrinology*. 1996;137(5):2109-2112.
31. Furigo IC, Teixeira PDS, de Souza GO, *et al.* Growth hormone regulates neuroendocrine responses to weight loss via AgRP neurons. *Nat Commun*. 2019;10(1):662.
32. Wasinski F, Barrile F, Pedroso JAB, *et al.* Ghrelin-induced food intake, but not GH secretion, requires the expression of the GH receptor in the brain of male mice. *Endocrinology*. 2021;162(7):bqab097.
33. Stilgenbauer L, de Lima JBM, Debarba LK, *et al.* Growth hormone receptor (GHR) in AgRP neurons regulates thermogenesis in a sex-specific manner. *Geroscience*. 2023;45(3):1745-1759.
34. Wasinski F, Furigo IC, Teixeira PDS, *et al.* Growth hormone receptor deletion reduces the density of axonal projections from hypothalamic arcuate nucleus neurons. *Neuroscience*. 2020;434:136-147.
35. Pan W, Yu Y, Cain CM, Nyberg F, Couraud PO, Kastin AJ. Permeation of growth hormone across the blood-brain barrier. *Endocrinology*. 2005;146(11):4898-4904.
36. Baltazar-Lara R, Zenil JM, Carranza M, *et al.* Growth Hormone (GH) Crosses the Blood-Brain Barrier (BBB) and induces neuroprotective effects in the embryonic chicken cerebellum after a hypoxic injury. *Int J Mol Sci*. 2022;23(19):11546.
37. Lein ES, Hawrylycz MJ, Ao N, *et al.* Genome-wide atlas of gene expression in the adult mouse brain. *Nature*. 2007;445(7124):168-176.
38. Steuernagel L, Lam BYH, Klemm P, *et al.* HypoMap-a unified single-cell gene expression atlas of the murine hypothalamus. *Nat Metab*. 2022;4(10):1402-1419.
39. Wasinski F, Pedroso JAB, Dos Santos WO, *et al.* Tyrosine hydroxylase neurons regulate growth hormone secretion via short-loop negative feedback. *J Neurosci*. 2020;40(22):4309-4322.
40. Chaves FM, Wasinski F, Tavares MR, *et al.* Effects of the isolated and combined ablation of growth hormone and IGF-1 receptors in somatostatin neurons. *Endocrinology*. 2022;163(5):bqac045.
41. Dos Santos WO, Wasinski F, Tavares MR, *et al.* Ablation of growth hormone receptor in GABAergic neurons leads to increased pulsatile growth hormone secretion. *Endocrinology*. 2022;163(8):bqac103.
42. Gusmao DO, de Sousa ME, Tavares MR, Donato J. Increased GH secretion and body growth in mice carrying ablation of IGF-1 receptor in GH-releasing hormone cells. *Endocrinology*. 2022;163(11):bqac151.
43. Bartolini P, Ribela MT. Influence of chloramine T iodination on the biological and immunological activity or the molecular radius of the human growth hormone molecule. *J Immunoassay*. 1986;7(3):129-138.
44. Nario AP, Woodfield J, Dos Santos SN, *et al.* Synthesis of a 2-nitroimidazole derivative N-(4-[(18)F]fluorobenzyl)-2-(2-nitro-1H-imidazol-1-yl)-acetamide ([(18) F]FBNA) as PET radiotracer for imaging tumor hypoxia. *EJNMMI Radiopharm Chem*. 2022;7(1):13.
45. Quaresma PGF, Dos Santos WO, Wasinski F, Metzger M, Donato J Jr. Neurochemical phenotype of growth hormone-responsive cells in the mouse paraventricular nucleus of the hypothalamus. *J Comp Neurol*. 2021;529(6):1228-1239.
46. Dos Santos WO, Juliano VAL, Chaves FM, *et al.* Growth hormone action in somatostatin neurons regulates anxiety and fear memory. *J Neurosci*. 2023;43(40):6816-6829.
47. Kastrup Y, Le Greves M, Nyberg F, Blomqvist A. Distribution of growth hormone receptor mRNA in the brain stem and spinal cord of the rat. *Neuroscience*. 2005;130(2):419-425.
48. Quaresma PGF, Teixeira PDS, Wasinski F, *et al.* Cholinergic neurons in the hypothalamus and dorsal motor nucleus of the vagus are directly responsive to growth hormone. *Life Sci*. 2020;259:118229.
49. Liddelow SA. Development of the choroid plexus and blood-CSF barrier. *Front Neurosci*. 2015;9:32.
50. Lai ZN, Emtner M, Roos P, Nyberg F. Characterization of putative growth hormone receptors in human choroid plexus. *Brain Res*. 1991;546(2):222-226.
51. Bartke A, Kopchick JJ. The forgotten lactogenic activity of growth hormone: important implications for rodent studies. *Endocrinology*. 2015;156(5):1620-1622.
52. Langlet F, Mullier A, Bouret SG, Prevot V, Dehouck B. Tanycyte-like cells form a blood-cerebrospinal fluid barrier in the circumventricular organs of the mouse brain. *J Comp Neurol*. 2013;521(15):3389-3405.
53. Faouzi M, Leshan R, Bjornholm M, Hennessey T, Jones J, Munzberg H. Differential accessibility of circulating leptin to individual hypothalamic sites. *Endocrinology*. 2007;148(11):5414-5423.
54. Noble EE, Hahn JD, Konanur VR, *et al.* Control of feeding behavior by cerebral ventricular volume transmission of melanin-concentrating hormone. *Cell Metab*. 2018;28(1):55-68e57.
55. Iliff JJ, Wang M, Liao Y, *et al.* A paravascular pathway facilitates CSF flow through the brain parenchyma and the clearance of interstitial solutes, including amyloid beta. *Sci Transl Med*. 2012;4(147):147ra111.
56. Fernandez G, De Francesco PN, Cornejo MP, *et al.* Ghrelin action in the PVH of male mice: accessibility, neuronal targets, and CRH neurons activation. *Endocrinology*. 2023;164(11):bqad154.
57. Nagaishi VS, Cardinali LI, Zampieri TT, Furigo IC, Metzger M, Donato J Jr. Possible crosstalk between leptin and prolactin during pregnancy. *Neuroscience*. 2014;259:71-83.
58. Furigo IC, Kim KW, Nagaishi VS, *et al.* Prolactin-sensitive neurons express estrogen receptor-alpha and depend on sex hormones for normal responsiveness to prolactin. *Brain Res*. 2014;1566:47-59.
59. Ramos-Lobo AM, Teixeira PD, Furigo IC, *et al.* Long-term consequences of the absence of leptin signaling in early life. *Elife*. 2019;8:e40970.
60. Tavares MR, Frazao R, Donato J. Understanding the role of growth hormone in situations of metabolic stress. *J Endocrinol*. 2023;256(1):e220159.
61. Langlet F, Levin BE, Luquet S, *et al.* Tanycytic VEGF-A boosts blood-hypothalamus barrier plasticity and access of metabolic signals to the arcuate nucleus in response to fasting. *Cell Metab*. 2013;17(4):607-617.

62. Posner BI, van Houten M, Patel B, Walsh RJ. Characterization of lactogen binding sites in choroid plexus. *Exp Brain Res*. 1983;49(2):300-306.
63. Zhai Q, Lai Z, Roos P, Nyberg F. Characterization of growth hormone binding sites in rat brain. *Acta Paediatr*. 1994;406(s406):92-95.
64. Kharchenko PV, Silberstein L, Scadden DT. Bayesian approach to single-cell differential expression analysis. *Nat Methods*. 2014;11(7):740-742.
65. Fink G. The external layer of the median eminence: a neurovascular synapse. *Neurochem Int*. 1986;9(1):141-153.
66. Wasinski F, Chaves FM, Pedroso JAB, *et al*. Growth hormone receptor in dopaminergic neurones regulates stress-induced prolactin release in male mice. *J Neuroendocrinol*. 2021;33(3):e12957.
67. Proescholdt MG, Hutto B, Brady LS, Herkenham M. Studies of cerebrospinal fluid flow and penetration into brain following lateral ventricle and cisterna magna injections of the tracer [14C]inulin in rat. *Neuroscience*. 2000;95(2):577-592.
68. Kelly PA, Djiane J, Postel-Vinay MC, Edery M. The prolactin/growth hormone receptor family. *Endocr Rev*. 1991;12(3):235-251.
69. Goffin V, Shiverick KT, Kelly PA, Martial JA. Sequence-function relationships within the expanding family of prolactin, growth hormone, placental lactogen, and related proteins in mammals. *Endocr Rev*. 1996;17(4):385-410.
70. Caron E, Sachot C, Prevot V, Bouret SG. Distribution of leptin-sensitive cells in the postnatal and adult mouse brain. *J Comp Neurol*. 2010;518(4):459-476.
71. Scott MM, Lachey JL, Sternson SM, *et al*. Leptin targets in the mouse brain. *J Comp Neurol*. 2009;514(5):518-532.